

# DESIGN IMPROVEMENTS OF A 2-DOF TRANSLATIONAL FLEXIBLE JOINT FOR FLEXIBLE COMPACT ARRAYS (FCA)

Gerwin Lapoutre<sup>(1)</sup>, Jos de Hoog<sup>(1)</sup>, Mathieu Robroek<sup>(1)</sup>, Martin Kroon<sup>(1)</sup>, Guus Borst<sup>(1)</sup>

<sup>(1)</sup> Airbus Netherlands B.V. Mendelweg 30, 2333 CS Leiden, The Netherlands

Email: [j.de.hoog@airbusds.nl](mailto:j.de.hoog@airbusds.nl), [m.robroek@airbusds.nl](mailto:m.robroek@airbusds.nl), [g.lapoutre@airbusds.nl](mailto:g.lapoutre@airbusds.nl), [m.kroon@airbusds.nl](mailto:m.kroon@airbusds.nl), [g.borst@airbusds.nl](mailto:g.borst@airbusds.nl)

## ABSTRACT

Airbus NL is developing a joint with flexibility in a 2 translational degree of (relative) freedom.

A first design, made by electro discharge machined Ti6Al4V, is tested and performs as expected in the two degrees of freedom.

A second design iteration was performed, with the goal of saving mass and costs. This is to be achieved by choosing a different material and manufacturing process, and by changing the interface. Finite Element Analysis shows that the bending stiffness is less than the first design iteration. A mass saving of 312g per unit is expected.

Development will continue with stiffness, fatigue, and strength testing.

## 1 CONTEXT

Airbus NL is developing – together with Airbus Defence & Space in Ottobrunn and Toulouse – a novel solar array, using a flexible carrier for the Photo Voltaic Assembly (PVA). This provides a higher specific power, compared to the conventional “rigid” solar array design, and increases the maximum power that can be delivered by a solar array. At the same time, this requires a new deployment mechanism, which is more complex compared to designs for classical rigid arrays.

The solar array consists out of 2 blanket stacks, a stack rotation mechanism (SRM), root hinge assembly (RHA) and a telescopic mast. Each blanket stack consists of 2 pressure plates, which contain the PVA in stowed configuration. Upon deployment, these pressure plates are first rotated 90° using the SRM. After 90° rotation of the blanket stack, the telescopic mast extends, allowing the solar array to deploy. This deployment sequence is shown in Fig. 1.

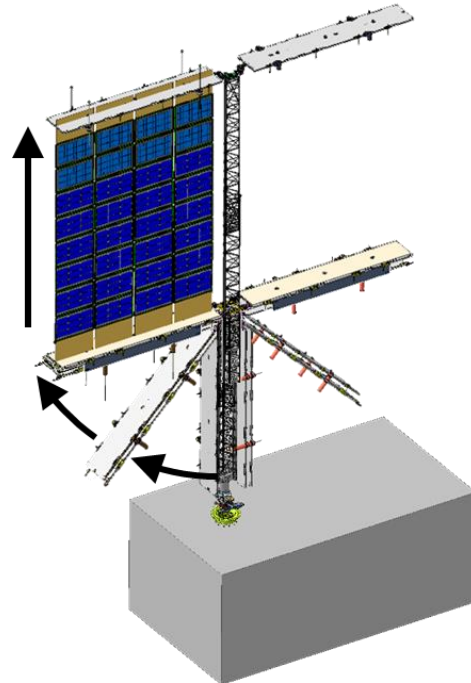


Figure 1 The Deployment Sequence of the Flexible Compact Array's Blanket Stack Rotation Mechanism

The Stack Rotation Mechanism (SRM) consists of 3 hinges per hinge line, one of which is connected to the upper pressure plate, and the other 2 attached to the bottom pressure plate. For the rotation of the SRM, the 3 separate hinge axes shall remain concentric to avoid rapid increase of hinge friction. Due to the tolerances of the bearing, manufacturing, and thermal expansion of the various components, the flexjoint is introduced. The flexjoint is to provide the required flexibility in 2 directions to limit the hinge friction, while also providing sufficient stiffness in the other 4 directions in order to satisfy deployed Eigenfrequency requirements. A 3D printed mock-up of the current design of the flexjoint is shown in Fig. 2.

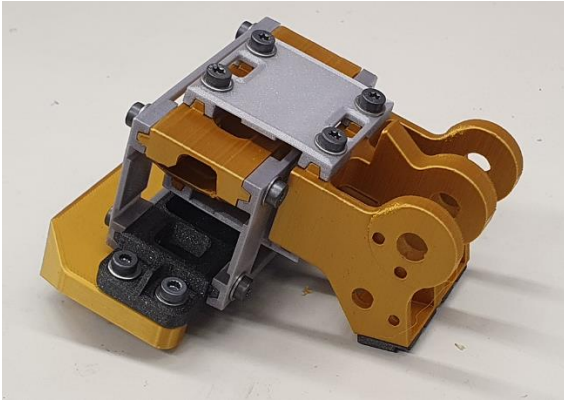


Figure 2 During the development of the flexjoint, 3D printing has been used frequently. The latest version of the flexjoint assembly is shown.

## 2 SYSTEM REQUIREMENTS

During operation of the SRM, the motorisation is provided by torque springs. In order to limit the required torque, and reduce corresponding negative effects on system level, a shear load exerted on the hinge of 140N is considered acceptable. In deployed configuration, the blanket is tensioned, and results in a load of 30Nm on the SRM. To assure a correct functioning of the mechanism, a set of requirements is defined. In terms of mechanical performance, the requirements are defined both for the SRM hinge mechanism and the flexjoint itself. The flexjoint requirements were used for defining the design of the first flexjoint design iteration. During the development of this mechanism, the requirements were updated, which resulted in the apparent mismatch between hinge requirements and flexjoint assembly requirements. The driving requirements for the design are shown in Sec. 2.1 up to 2.3

### 2.1 Hinge mechanical

- The hinge stiffness shall comply with the following requirements
  - $K_{xx} > 1 \text{ kNm/rad}$
  - $K_{yy} > 2 \text{ kNm/rad}$
  - $K_{zz} > 2,3 \text{ kNm/rad}$

### 2.2 Flexjoint Mechanical

- The flexjoint shall comply with the following stiffness requirements
  - $K_x > 10 \text{ kN/mm}$
  - $50 \text{ N/mm} < K_y < 140 \text{ N/mm}$  (within a displacement of  $\pm 1 \text{ mm}$ )
  - $50 \text{ N/mm} < K_z < 140 \text{ N/mm}$  (within a displacement of  $\pm 1 \text{ mm}$ )
  - $K_{xx} > 10 \text{ kNm/rad}$
  - $K_{yy} > 2 \text{ kNm/rad}$
  - $K_{zz} > 2 \text{ kNm/rad}$

- The  $K_y$  and  $K_z$  requirements are derived from a simple friction test on the hinge bearing with an applied force perpendicular to the rotation axis. The resulting friction still fits within a motorisation factor of 3. The displacement requirement of  $\pm 1 \text{ mm}$  results from a tolerance analysis of the SRM using Monte-Carlo analysis with a confidence level of  $>99\%$  (i.e.,  $<1\%$  chance that a part has to be replaced in order to pass the acceptance test).

### 2.3 Design

- The flexjoint should fit inside a volume of  $80 \times 50 \times 42 \text{ mm}$
- The flexjoint should interface to the hinge line bracket using 4 bolts with a  $60 \times 23 \text{ mm}$  pattern
- The flexjoint should interface to the pressure plate bracket using 4 bolts with a  $15.5 \times 22.5 \text{ mm}$  pattern
- The flexjoint mass target is  $<400 \text{ g}$

## 3 FIRST ITERATION

The design of the first iteration was outsourced. The requirements for this development are listed in Sec. 2.2. The design, as shown in Fig. 3, consists of 2 sets of flexures, allowing for the required 2 degrees of relative freedom, while remaining stiff in the other 4 directions. The main parts are manufactured using electrical discharge machining (EDM) out of Ti6Al4V. Bolts are used to connect the various SRM components to each other, and to interface with the SRM.

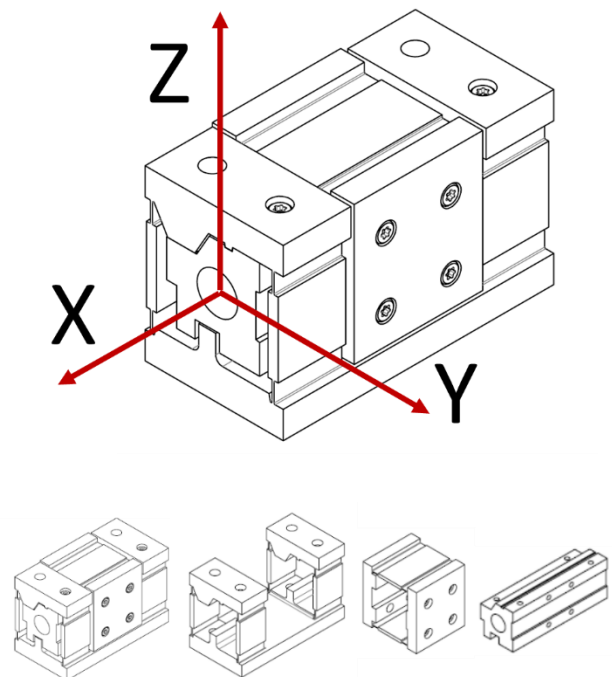


Figure 3 The different components of the Flexjoint first version

### 3.1 Analytical Flexure Model

The stiffness is calculated analytically using Eqs 1 to 5. for a single element, as shown in Fig. 4.

$$C_x = \frac{1}{2\lambda(1-\gamma)+\gamma} \cdot \frac{Etb}{L_0} \quad (1)$$

$$C_y = \frac{1}{2\lambda(4\lambda^2-6\lambda+3)(1-\gamma)+\gamma} \cdot \frac{Etb^3}{L_0^3} \quad (2)$$

$$C_z = \frac{1}{2\lambda(4\lambda^2-6\lambda+3)(1-\gamma^3)+\gamma^3} \cdot \frac{Et^3b}{L_0^3} \quad (3)$$

$$\lambda = \frac{L_s}{L_0} \quad (4)$$

$$\gamma = \frac{t}{T} \quad (5)$$

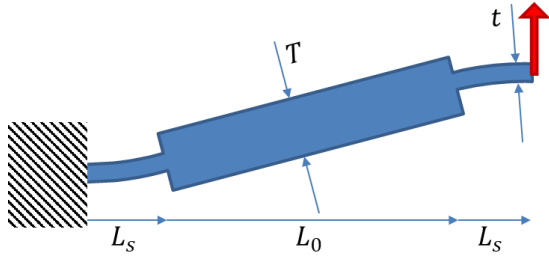


Figure 4 A single Flexure Element [1], with important dimensions indicated.

Combining eqs 1-5 with the dimensions as defined in Tab. 1 results in an analytical stiffness as presented in Tab.2

Table 1 Design parameters of flexjoint

Parameter	Flex Y	Flex Z
E	196 [GPa]	196 [GPa]
t	0.4 [mm]	0.4 [mm]
b	14 [mm]	40 [mm]
L <sub>0</sub>	26 [mm]	26 [mm]
γ	0.25	0.25
λ		

Table 2 Analytical stiffness of system, based on flexure stiffness values only

Direction	Analytical stiffness
C <sub>x</sub>	16900 [N/mm]
C <sub>y</sub>	33 [N/mm]
C <sub>z</sub>	66 [N/mm]
K <sub>xx</sub>	45,2 [kNm/rad]
K <sub>yy</sub>	9,61 [kNm/rad]
K <sub>zz</sub>	21,0 [kNm/rad]

### 3.2 Finite Element Flexure Model

The design has been analysed using Nastran. The analytical model only took into account the stiffness of the blades. The interfacing brackets between the different flexures cannot be considered rigid, but have not been included in the analytical model. The effect of neglecting flexibility in these parts is most pronounced in the directions with high stiffness.

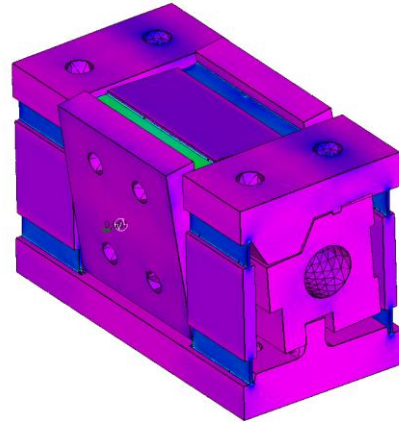


Figure 5 FEM results for Von Mises stresses as a result of an applied bending moment around the x-axis

Table 3 Comparison between analytical stiffness values, calculated using flexure stiffness values only, and FEM calculation

Direction	Analytical stiffness	FEM prediction
C <sub>x</sub>	16900 [N/mm]	7596
C <sub>y</sub>	33 [N/mm]	39
C <sub>z</sub>	66 [N/mm]	73
K <sub>xx</sub>	45,2 [kNm/rad]	27,1
K <sub>yy</sub>	9,61 [kNm/rad]	6,33
K <sub>zz</sub>	21,0 [kNm/rad]	9,97

### 3.3 Validation of Flexjoint

The flexjoint stiffness is tested for translational stiffnesses C<sub>y</sub>, C<sub>z</sub>, and bending stiffness K<sub>x</sub>. The translational stiffness has been measured between -1mm and +1mm with respect to the neutral position. The bending stiffness has been measured while cycling between -30 Nm and +30 Nm.

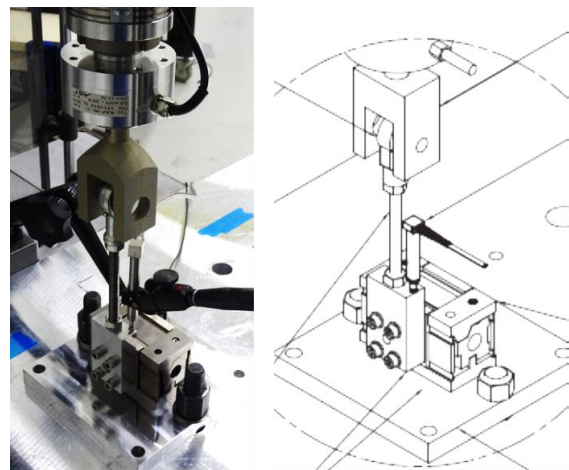


Figure 6 Testing of the flexjoint in y-direction. Force is measured using a load cell located in line with the applied load, and displacement is measured using a LVDT applied at the interface bracket

Direction	Fem Prediction	Test SN01	Test SN02
$C_x$ [N/mm]	7596	-	-
$C_y$ [N/mm]	39	38,7	38,2
$C_z$ [N/mm]	73	75,8	72,9
$K_{xx}$ [kNm/rad]	27,1	18,0	14,8
$K_{yy}$ [kNm/rad]	6,33		
$K_{zz}$ [kNm/rad]	9,97		

The mass of the flexjoint measured 543g.

Differences between the FEM prediction and test results are small for the intended degrees of freedom, but larger for the bending stiffness. It is expected that the difference on bending stiffness between the FEM and the tested values is caused by the effect of the mounting interfaces.

#### 4 SECOND ITERATION

With the results of the first flexjoint, there was room for improvement, which was to be tackled by a second design iteration.

The first iteration of the flexjoint resulted in a design which met the requirements in terms of stiffness. The mass exceeded the target, and the decision to go with Ti6Al4V in combination with EDM was deemed unwanted. The flexures are subjected to cyclic loading during launch. It is known that fatigue life of EDM machined titanium components can vary with supplier, and machine settings [2]. This would require additional effort in the qualification of the flexjoint.

The design of a second iteration of the flexjoint was initiated in order to reduce the mass, recurring and non-recurring cost. The design activities were performed in-house, allowing a better integration of interfaces with surrounding components.

Stainless steel was chosen as flexure material for the second iteration. All other parts are made of Aluminium 7075. This allowed for manufacturing of the flexure using milling; resulting more predictable fatigue life, increase in potential suppliers, and a decrease in associated manufacturing cost. A sample has been machined to prove that tolerances specified are achievable.

The flexures interface directly with the hinge bracket, cross bracket, and panel interfacing bracket, using a groove interface. The groove interface is bolted using M4 bolts. Overloading of the flexures is prevented using a pin which makes contact when a travel of  $\pm 1,1$ mm is achieved.

The mass of the flexjoint components is 253g, where the flexjoint is defined as the 4 flexures, the central part, the hinge bracket, and the interfacing bracket on opposite side. Combined with modifications on other components of the SRM results in a total mass savings per hinge side of 312g.

##### 4.1 Analytical Flexure Model

The 2<sup>nd</sup> version of the flexjoint, using the same members

as the first version, uses the same analytical model to arrive at the expected stiffness. The resulting stiffness values are presented in Tab. 4

Table 4 The analytical stiffness found, using Eqs. 1 to 5

Direction	Analytical stiffness
$C_x$	24214 [N/mm]
$C_y$	60 [N/mm]
$C_z$	61 [N/mm]
$K_{xx}$	58,3 [kNm/rad]
$K_{yy}$	29,8 [kNm/rad]
$K_{zz}$	11,9 [kNm/rad]

From the previous iteration, it is expected that a knock down has to be applied in order to come from the analytical model predicted values to the FEM predicted values. An additional knock down is to be applied when going from the FEM predicted value to the actual measured values.

##### 4.2 Finite Element Flexure Model

The second design iteration also included an update of the flexure interfaces and hinge brackets. The interfaces and brackets have been optimized, which will result in a different behaviour compared to the previous iteration. Two models were created, one assessing the behaviour of the mechanism as a whole, and one model to study the effect of the bolted groove interface. The models were created using Abaqus, and contact between the interfaces is modelled using surface-to-surface contact. The coefficient of friction was set at 0.45, and once the contact was initiated, it was not allowed to open ("hard contact").

Table 5 Comparison between analytical stiffness values, calculated using flexure stiffness values only, and FEM calculation

Direction	Analytical stiffness	FEM prediction
$C_x$	24214 [N/mm]	3370 [N/mm]
$C_y$	60 [N/mm]	59 [N/mm]
$C_z$	61 [N/mm]	57 [N/mm]
$K_{xx}$	58,3 [kNm/rad]	7,0 [kNm/rad]
$K_{yy}$	29,8 [kNm/rad]	2,8 [kNm/rad]
$K_{zz}$	11,9 [kNm/rad]	5,9 [kNm/rad]

The predicted values for the stiff directions are lower than expected based on the previous design iteration. After assessing the interfaces in more detail, it is expected that the interface is culprit to the low stiffness values. It can be seen in Fig. 7 and Fig. 8 that the groove interface of the flexjoint is highly stressed after applying the bolt preload. After applying an additional bending load, the interface shows even higher stresses, and clear signs of deformation. This weak part of the interface is affecting the flexjoints stiffness characteristics.



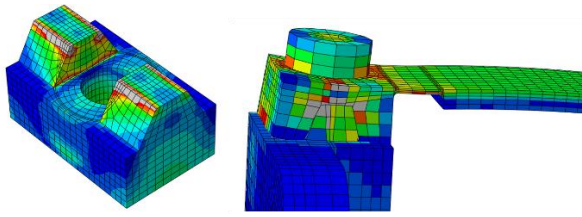


Figure 7 The result of pretensioning the bolted groove interface (shown left) and resulting stresses after applying a bending load on the flexjoint assembly (right). It can be seen that the groove interface seems to open upon loading.

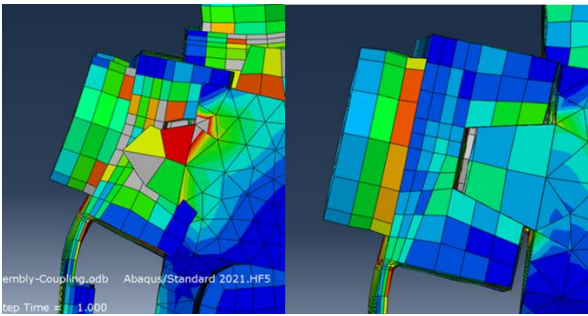


Figure 8 The effect of the interface has been studied in more detail. On the left, contact with friction has been modelled. On the right, the contact has been fixed, creating a stiff connection, resulting in an increase in bending stiffness of 31%

The geometry of the flexures might also contribute to a decrease in stiffness characteristics. Due to machinability, the reinforcement areas are only on one side of the bending element. When compressed, the reinforcement area tends to deform out of plane, while a symmetric reinforcement area is expected to only start deforming out of plane after buckling. Both sources of unwanted flexibility can be reduced by adding thickness to the interface element or to the reinforced area of the blade.

## 5 FUTURE

With FEM analysis completed, the next phase can start. The performance of the SRM is to be determined, using the updated flexjoint, and the improvements made on other components of the mechanism.

The performance of the flexjoint is to be tested in the y- and z-direction, and the bending stiffness around the x-axis, verifying the stiffness parameters of interest. The flexjoint will also be subjected to a fatigue test, as the flexjoint vibrates within its intended range during launch. The strength of the flexjoint is determined in an ultimate bending load test, after fatigue, to verify whether the intended margins of safety are met.

It is expected that with the completion of these activities, the performance of the flexjoint and hinge assembly are known.

## 6 LESSONS LEARNED

During the development of the flexjoint and Stack

Rotation mechanism, the following lessons would have helped us develop the mechanism more effectively;

- By applying the leaf spring equations, the stiffness for the DoF of interest can be estimated quickly and accurately
- Interfaces are important; If not properly designed, an interface can result in significant mechanical performance losses
- The machining process dictates what tolerances can be achieved, and vice versa. Generating a 'robust' design can allow for manufacturing processes with a better availability, less complexity, and less cost.

## 7 CONCLUSIONS

Airbus NL has successfully tested a first version of a 2 translational degree of freedom flexible mechanism, with a stiffness of 38 N/mm in y-direction, and a stiffness of 73 N/mm in z-direction, while maintaining a high bending stiffness of 14,8 kNm/rad. The second iteration of this flexible mechanism – internally called flexjoint – is expected to result in a weight saving on hinge level of 312g.

This is achieved by taking control over the interfaces, and optimizing the components for weight, while keeping manufacturability of components key. As a result, a switch was made from Ti6Al4V with electric discharge machining to stainless steel milled flexures. After performing Finite Element Analysis on the second design iteration, the predicted stiffness was lower than anticipated. This is possibly caused by groove interface, which is too thin, and highly stressed.

Development continues with testing of the stiffness, fatigue behaviour and strength of the flexjoint.

## 8 REFERENCES

1. JPE – LEAF SPRING/FLEXURE: REINFORCED Online at <https://www.jpe-innovations.com/precision-point/leaf-spring-flexure-reinforced/> (accessed 30-06-2023)
2. Puyol, Y., Blecha L., Humphries M., Hayoz S., Rottmeier F., (2019) Innovation in Large Angle Flexible Pivot Design & Material accelerated Fatigue Screening Tests Results. In Proc. 18<sup>th</sup> European Space Mechanisms and Tribology Symposium, ESA